

Modeling of three-dimensional velocity field in open channel flows

Modélisation des champs de vitesses tridimensionnelles en canal à surface libre

W. CZERNUSZENKO, *Professor, Polish Academy of Sciences, Institute of Geophysics, Ks. Janusza 64, 01-452 Warsaw, Poland*

A. RYLOV, *Dr., Institute for Water & Environmental Problems, 105 Papanintsev Street, Barnaul 656099, Russia*

ABSTRACT

A comparatively simple model for calculation of the three-dimensional, stationary velocity field is presented. The model is able to calculate the streamwise velocity distribution as well as the secondary flow in a cross-section of regular channel. The Reynolds equations are closed by a new anisotropic turbulence model which consists of two sub-models: one for the shear stresses and the other for normal stresses. The numerical solution of the parabolic approximation of the model equations gives reasonably good secondary flow patterns as well as the longitudinal velocity distribution in the channel cross-section.

RÉSUMÉ

Un modèle relativement simple pour le calcul en trois dimensions du champ stationnaire des vitesses est présenté. Ce modèle permet de calculer la distribution de la composante longitudinale de la vitesse ainsi que le courant secondaire dans une section rectangulaire. Les équations de Reynolds sont fermées à l'aide d'un nouveau modèle anisotrope de la turbulence constitué de deux sous-parties; la première pour les contraintes de cisaillement et la seconde pour les contraintes normales. La solution numérique de l'approximation parabolique du modèle d'équations donne des résultats satisfaisants pour le courant secondaire ainsi que pour la distribution de la vitesse longitudinale dans la section du canal.

Introduction

Calculations of the three-dimensional (3D) velocity field in open channel flows are based on the solution of the Reynolds equations closed by a turbulence model. Many turbulence models, from simple to very complicated ones, are available at present. Most of them are two-equation models, which incorporate the so called transport equation for the kinetic energy of turbulent motion k and the dissipation rate of this energy ε . Besides the mixing length hypothesis (MLH), the k - ε model is likely to be the most widely tested and successfully applied in hydraulics. The standard k - ε model is based on the assumption of isotropic eddy viscosity, i.e., at any point of the flow the eddy viscosity is the same for all Reynolds stress components. The assumption of local isotropy in flow is not corroborated at low Reynolds numbers, i.e., anisotropic effects cause that high Reynolds number models predict the shear stress field very poorly [11]. Calculations of the longitudinal velocity component in wide open channels are not influenced by accepting or rejecting this assumption of local isotropy because only the shear stress is important in this kind of flow. Calculations of other flows, like vertical and surface flow jets, side discharges, or recirculation flows, in which the normal and shear stresses are small in comparison with inertial and pressure terms, do not depend on this assumption either. However, there are flows for which the assumption of isotropic eddy viscosity cannot be accepted, for example, an open channel flow with secondary currents.

The turbulent secondary flows in 3D open channels are closely related to the streamwise mean vorticity. Gerard [3] pointed out that the mechanism of secondary flow creates the mean stream vorticity in open channel flows. Streamwise mean vorticity can be generated, for example, by lateral deflection or 'skewing' of

preexisting shear layers [1]. This kind of mechanism is called 'skew-induced' or 'secondary currents of Prandtl's first kind'. It appears in the transport equation for the x -wise mean vorticity (Eq.1) as the second and third terms on the right-hand side of the equation.

$$U \frac{\partial \Omega_x}{\partial x} + V \frac{\partial \Omega_x}{\partial y} + W \frac{\partial \Omega_x}{\partial z} = \Omega_x \frac{\partial U}{\partial x} + \Omega_y \frac{\partial U}{\partial y} + \Omega_z \frac{\partial U}{\partial z} + \frac{\partial}{\partial x} \left(\frac{\partial \overline{uv}}{\partial z} - \frac{\partial \overline{uw}}{\partial y} \right) + \left(\frac{\partial^2}{\partial y^2} - \frac{\partial^2}{\partial z^2} \right) (-\overline{vw}) + \frac{\partial^2}{\partial y \partial z} (\overline{v^2} - \overline{w^2}) + \nu \nabla^2 \Omega_x \quad (1)$$

where: U, V, W are components (longitudinal, vertical and lateral) of mean velocity vector, u, v, w are components of the turbulent velocity, $\Omega_x, \Omega_y, \Omega_z$ are components of mean vorticity vector, ν is kinematic viscosity.

The skewing is mainly caused by lateral gradient of streamline velocity. Since Ω_y is close to zero, at least initially, then $\partial U / \partial z$ is equal to $\partial W / \partial x$, and the streamwise vorticity can also be said to arise from the latter [1]. The skew-induced mechanism can be found in both laminar and turbulent flows, but it does not exist in uniform, fully-developed turbulent flows in open channels where the sum of second and third terms of Eq.1 is close to zero. In these flows streamwise mean vorticity can actually be generated by the turbulence (Reynolds) stresses. This kind of secondary flow is called secondary currents of Prandtl's second kind or the stress-induced secondary currents. It can be found in 3D free jets, wall jet as well as in flows in ducts and open channels. Equation (1) for fully-developed turbulent flows in open channels reduces to the form:

Revision received January 22, 2001. Open for discussion till August 31, 2002.

$$V \frac{\partial \Omega_x}{\partial y} + W \frac{\partial \Omega_x}{\partial z} = \left(\frac{\partial^2}{\partial y^2} - \frac{\partial^2}{\partial z^2} \right) (-\overline{vw}) + \frac{\partial^2}{\partial y \partial z} (\overline{v^2} - \overline{w^2}) + v \nabla^2 \Omega_x \quad (2)$$

In channels, the differences between intensities of turbulence in lateral and vertical directions are large near a solid surface because one of these intensities reduces to zero at the surface. This results in an increase of the second term on the right-hand side of Eq.2. Many researchers are convinced that the anisotropy of the transverse normal Reynolds stresses is responsible for the generation of secondary flows. However, some measurements indicate, on the contrary, that the normal Reynolds stresses do not have a dominant role in the generation of the secondary currents, but instead, this flow exists primarily due to Reynolds shear stress gradients in the corner region [5]. On the other hand, Perkins [10] showed that two turbulent stresses were in balance, over the majority of the cross section, with the convective term becoming significant near the corner and the viscous term – very near the wall.

Gessner [4] showed that transverse gradients of Reynolds shear stress components, which influence the streamwise shear characteristics of the primary flow, were directly responsible for the generation of secondary flow in turbulent flow along a corner. This secondary flow acts as a convective transport mechanism in the plane normal to the primary-flow direction. The secondary flow transfers momentum and vorticity of the primary flow, as well as the total energy of the mean motion.

The main aim of the paper is to provide engineers with a relatively simple model for calculation of 3D velocity field in open channels including the secondary motion. The model is based on the Reynolds equations and a new turbulence model. In fact, there are two models for turbulent stresses: one for shear stresses and the other for normal stresses. The first model stems from the 3D MLH of Czernuszenko and Rylov [2], and the second one dealing with the normal stresses incorporates empirical formulae based on quite precise measurements of turbulent quantities. The paper attempts to clarify a role of the shear and normal Reynolds stresses in creating the patterns of secondary currents and streamwise velocity in the cross section of open channel flows. It also shows that sizes of turbulent eddies, in different directions, may be associated with the components of the mixing length tensor.

Mean-flow equation

The continuity and momentum equations for incompressible turbulent flows may be written in the Cartesian tensor notation as follows:

– continuity equation

$$\frac{\partial U_i}{\partial x_i} = 0 \quad (3)$$

– momentum equation

$$\rho \frac{DU_i}{Dt} = \frac{\partial}{\partial x_j} \sigma_{ij} + F_i \quad (4)$$

where U_i is the i -th component of the average velocity ($i=1,2,3$), $\mathbf{F}=(0,\rho g,0)$, and the substantive derivative, $D/Dt=\partial/\partial t+U_i\partial/\partial x_i$. A notation of x for horizontal (longitudinal), y for vertical (downwards) and z for lateral coordinates as well as U, V, W for corresponding velocity components will be used further in the paper. The stress tensor for the turbulent flow can be written as follows

$$\sigma_{ij} = -p\delta_{ij} + \mu D_{ij} - \overline{\rho u_i u_j} \quad (5)$$

where p is an average pressure, D_{ij} is a deformation rate tensor

$$D_{ij} = \frac{\partial U_i}{\partial x_j} + \frac{\partial U_j}{\partial x_i} \quad (6)$$

in which u_i is the i -th component of the turbulent velocity, the overbar denotes a time-average quantity and $-\overline{\rho u_i u_j}$ is known as the Reynolds stress tensor or the turbulent stress tensor. It is a symmetrical tensor with six independent components. The ways of determination of these components allowing to solve Eqs.3-6 are called the turbulence models. The simplest turbulence models employ the Boussinesq eddy-viscosity approximation to compute the Reynolds stresses as the product of an eddy viscosity coefficient and the deformation tensor. For computational simplicity, the eddy viscosity is, in turn, often computed in terms of the mixing length that is analogous to the mean free path of molecules in the kinetic theory of gases. Prandtl's mixing length hypothesis (MLH) is among the simplest turbulence models for modeling the turbulent shear stress. Unfortunately, Prandtl's MLH does not include any information on the normal turbulent stresses. For homogeneous turbulence, the normal turbulent stresses are usually included into pressure and they do not have to be calculated. This is not the case, because a turbulent flow in open channels is usually not homogeneous. Thus, in addition to specifying shear stresses, modeling of turbulent normal stresses is needed. This problem is discussed below.

Turbulence model

The Reynolds equations for incompressible turbulent flows incorporate the components of the turbulent stress tensor, which can be decomposed into a sum of two tensors, i.e., the tensor of turbulent normal stresses and the tensor of turbulent shear-stresses, respectively:

$$\overline{u_i u_j} = \begin{vmatrix} \overline{u_1^2} & 0 & 0 \\ 0 & \overline{u_2^2} & 0 \\ 0 & 0 & \overline{u_3^2} \end{vmatrix} + \begin{vmatrix} 0 & \overline{u_1 u_2} & \overline{u_1 u_3} \\ \overline{u_1 u_2} & 0 & \overline{u_2 u_3} \\ \overline{u_1 u_3} & \overline{u_2 u_3} & 0 \end{vmatrix} \quad (7)$$

The density multiplier is omitted in Eq.7 merely for convenience. Components of the above-mentioned tensors will be defined in two different areas (zones) of an open channel: the middle zone and the edge zone (see Fig.1). The middle zone is located far away from the vertical channel walls where assumptions of a two-dimensional approximation could be accepted. Thus, the edge zones take into account the side wall influence, and the middle zone represents the part of the channel where Prandtl's hypothesis is justified.

Tensor of Turbulent Shear Stresses

A model for shear stresses is defined by generalization of a simple mixing length hypothesis (MLH) proposed by Prandtl. Despite its simplicity, the Prandtl model proved to be very fruitful in many problems of turbulence description. It was formulated for unidirectional two-dimensional turbulent flows over a wall in the case when velocity depends only on a distance from the wall. The turbulent shear stress in such a flow takes the form

$$-\overline{\rho v u} = \rho l^2 \left| \frac{du}{dy} \right| \frac{du}{dy} \equiv \rho v_t \frac{du}{dy} \quad (8)$$

in which ρ is the density and l is Prandtl's mixing length. The mixing length hypothesis has been applied to flows in open channels with a great success for many years. Much experience of using the MLH has been accumulated and is available through publications. Advantages and disadvantages of the MLH are well known. The mixing length distribution over depth in 2D fully developed turbulent flows is well described by the Nikuradse formula. It has been used by civil engineers for many years in the form [13]:

$$\frac{1}{h} = 0.14 - 0.08(1 - \xi)^2 - 0.06(1 - \xi)^4 \equiv 0.14 N_i(\xi) \quad (9)$$

where $\xi = (h-y)/h$, h = water depth, y = distance from the water surface; the introduced function $N_i(\xi)$ maps segment $[0,1]$ onto itself. The formula can also be applied to calculate the mixing length in the lateral direction. Then the depth should be replaced by the half width of the channel, $B/2$, and ξ by non-dimensional distance from the side wall [12]. However, the formula gives too large lateral mixing lengths for wide channels; therefore, the half width should be replaced by a distance that represents the influence of the side wall.

Nezu and Rodi [9] published the results of measurements of the mean flow and turbulence structure in an open channel flow with the aid of the highly accurate two-color LDA system. They obtained the following formula for the mixing length that can be easily deduced from the log-wake law for the mean velocity

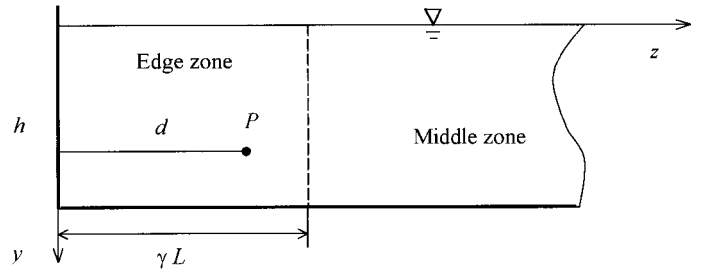


Fig. 1. The rectangular channel cross section.

$$\frac{1}{h} = \kappa \sqrt{1 - \xi} \left(\frac{1}{\rho} + \pi \Pi \sin(\pi \xi) \right)^{-1} \equiv L_w(\xi) \quad (10)$$

where κ is von Karman's constant and Π is Coles' constant. Formulae (9) and (10) for the mixing lengths have been proved to be satisfactory, i.e., when they are used as a closure for Reynolds equations, the obtained vertical velocity distributions in 2D turbulent flow match the experimental data well. It is easy to notice that these formulae are quite different in the area close to a water surface. According to the Nikuradse formula the mixing length grows from zero at the channel bottom to maximum value of $0.14h$ at the water surface. The Nezu and Rodi formula gives almost the same maximum value but at the distance from the channel bottom equal to $2h/3$. Differences between these formulae occur in the area near the water surface where the gradient of velocity is close to zero, so these differences do not produce different velocity distributions.

It is worth to note that Eq.9 and Eq.10 can be interpreted as the relation between the mixing length and the vertical size of the largest turbulent eddies that can exist in open channel flows. The vertical size of the largest turbulent eddies cannot be larger than the flow depth and usually is taken equal to the flow depth. Therefore, Eq.9 and Eq.10 show that the mixing length depends on the size of largest turbulent eddies and it is vertically distributed according to the scaling functions, i.e. $N_i(\xi)$ or $L_w(\xi)$. The largest mixing length can be estimated from Eq.9 at $\xi=1$ as equal to $0.14h$. Since the mixing length vanishes at the wall, it ranges from zero to $0.14h$ and the average size of turbulent eddies range from zero to the flow depth. The same range of the mixing length can be obtained from Eq.10.

In three-dimensional flows the mixing length appears to be the second rank tensor (l_{ij}) rather than a scalar value [7]. It allows the mixing length to vary in different space directions. Hence Eq.8 may be generalized to give turbulent shear stresses different in main three directions. Details of the generalization of Prandtl's MLH for 3D turbulent flows are given in [2], where one can find the final equation for components of turbulent shear stresses in the form:

$$-\overline{\rho u_i u_j} = \frac{1}{2} \rho \left(l_{ik}^2 D_{kj} + l_{jk}^2 D_{ki} \right) S, \quad i \neq j \quad (11)$$

where D_{ij} is the deformation rate tensor, S is defined by the formula [2]:

$$S = \sum_{ij} \left| \frac{\partial U_i}{\partial x_j} \right| \quad (12)$$

For the open channel flows the right-hand sum in this formula may be reduced to two terms containing derivatives of streamwise velocities in lateral and vertical directions, respectively. This is possible because lateral and vertical components of flow velocity do not exceed 1-2% of the streamwise component. Eq.11 can be applied to calculate the shear stresses in Prandtl's flow, for which the MLH was originally developed.

$$-\overline{\rho u_x u_y} = \frac{1}{2} \rho (l_{xx}^2 + l_{yy}^2) \left| \frac{dU}{dy} \right| \quad (13)$$

The above formula differs from the original Prandtl's one (Eq.8), but it is easy to notice that when the mixing lengths in longitudinal and vertical directions are equal these formulae also become identical. A general condition for coincidence of formulae(8) and (13) can be easily deduced by comparing the right-hand sides of these equations. It reads

$$l^2 = 0.5 (l_{xx}^2 + l_{yy}^2) \quad (14)$$

Mixing length tensor

Assuming that the main axes of mixing length tensor are directed along the coordinate directions, the tensor becomes diagonal and only three non-zero components: l_{11} , l_{22} , and l_{33} remain. Below, these three components are referred to as l_x , l_y , and l_z , respectively. Formulae Eq.9 and Eq.10 for the mixing length are justified for the two-dimensional turbulent flows, i.e., in the middle zone of the channel, far away from the side walls. Now the mixing length in Eq.9 and Eq.10 can be treated as an apparent 2D mixing length related to longitudinal and vertical mixing lengths by Eq.14.

A generic mixing length will be defined as an analogue of Prandtl's mixing length in the whole cross-section of a channel. It will be assumed that in the middle zone of a channel the mixing length depends only on the distance from the bed, and while in the edge zone it depends also on the distance from the side wall. The generic mixing length within the whole cross-section of a channel is defined as follows

$$l_{3D} = A(d)Lw(\xi), \quad A(d) = \begin{cases} L Ni\left(\frac{d}{\gamma L}\right), & \text{if } \frac{d}{\gamma L} < 1 \\ L, & \text{else} \end{cases} \quad (15)$$

where d stands for the z -distance from the side wall as shown in Fig.1, $A(d)$ has a dimension of length and can be considered as the greatest size of turbulent eddies at the given vertical (here the size is related to 2D case of Prandtl). In the middle zone $A(d)$ is equal to L , and due to Yalin [15] L may be assumed as equal to the depth, h . In this zone the generic mixing length becomes the

apparent 2D mixing length, and it varies in vertical direction according to Eq.10. It can be decomposed into two mixing lengths, longitudinal and vertical, as shown in Eq.14. In the edge zone, the maximum size of the generic mixing length varies according to the Nikuradse function $Ni(d)$. It is equal to zero at side walls and reaches its maximum at the boundary vertical between edge and middle zones. The lateral position of the boundary between the middle zone and the edge zone is assumed to be equal to L multiplied by the empirical coefficient γ .

Based on the generic mixing length the main components of the mixing length tensor can be defined in the following way:

$$l_x = p l_{3D}, \quad l_y = q_y l_x, \quad l_z = q_z l_x \quad (16)$$

where p , q_y and q_z are empirical, positive coefficients. Bearing in mind that Eq.11 should reduce to Prandtl's formula (Eq.8) in the middle zone of the channel, we get constraints on above mentioned coefficients

$$p^2 (1 + q_y^2) = 2, \quad p < \sqrt{2} \quad (17)$$

Measurement data shows that turbulent eddies in open channel flows are extended in longitudinal direction, so one can expect $q_y < 1$ and $p > 1$. Eqs.(16-17) allow us to estimate the components of the mixing length tensor when the generic mixing length as well as the two coefficients p or q_y and q_z are known.

One can assume that the relation between l_{3D} and the size of the largest turbulent eddies exists and it is expressed by Eq.15. Thus, the decomposition of l_{3D} into three main components of the mixing length tensor gives in turn, the decomposition of one size turbulent eddy into 3D ellipsoid eddies. The decomposition means that the circle (ring) eddy in Prandtl's approach becomes ellipse eddy in 2D flow or ellipsoid in 3D case. Summarizing, the largest turbulent eddies in open channel flows are ellipsoids with main axes equal to pL in longitudinal, $p q_y L$ in vertical and $p q_z L$ in lateral direction, respectively. Comparing the above relations and those defined by Eq.16, it is easy to notice, that ratios between mixing lengths i.e., $l_i:l_j$ are equal to counterpart ratios of sizes of the largest turbulent eddies i.e., $L_i:L_j$, for $i,j=1,2$ and 3.

Tensor of Turbulent Normal Stresses

A model for turbulent stresses needs to be specified in the middle zone as well as in the corner regions of an open channel. Components of the normal turbulent stresses, for the middle zone of an open channel, are taken from measurements. Nezu and Nakagawa [8] published results of measurements of turbulence intensities (rms of turbulent velocities) in a two-dimensional, fully-developed open channel flow. These results for turbulence intensities were averaged and approximated by the exponential law over the depth in the following forms:

$$\frac{u'_{i,2D}}{U_*} = D_i \exp(-C_k \xi) \quad (18)$$

in which D_i ($i=1,2,3$) and C_k are empirical constants, u_i' ($i=1,2,3$) are intensities of turbulence in longitudinal, vertical and lateral direction, respectively. The precise measurements by hot-film anemometry in smooth open channel flows allow us to evaluate the empirical constants in equations 18 as follows: $C_k=1$, $D_1=2.30$, $D_2=1.27$ and $D_3=1.63$. These values proved to be independent of the Reynolds and Froude numbers [8]. Eqs.(18-20) with above-mentioned coefficients fit the measurement data quite well, especially in the region $0.1 < \xi < 0.8$. Also, these equations fit measuring data from channels with rough beds but the lower limit of the region equals to 0.3. It is worth to note that the longitudinal intensity is larger than transversal ones and suitable ratios are: $v'/u'=0.55$ and $w'/u'=0.71$.

Components of the normal turbulent stresses in the edge zones of an open channel were measured by Tominaga, Nezu, Ezaki, and Nakagawa [14]. The measurements were conducted in the developed turbulent flow in smooth, rectangular, tilting flume with 12.5 m length and 40 cm x 40 cm cross-section. These authors examined 3D turbulent structure using an X-type hot-film probe. Parameters of relevant runs are summarized in Tab1. They presented the formulae for $\sqrt{v'^2}$ and $\sqrt{w'^2}$ that fit their measurements in the open channel whose ratio of width B to depth h equals 2. These formulae are verified and calibrated by authors for available data and their final stage are

$$v' = U_* \left(A_{vy} - B_{vy} Y^2 \right)^{\frac{Z}{Y+Z}} \left(A_{vz} e^{-B_{vz} Z} \right)^{\frac{Y}{Y+Z}} f_v(Y) \quad (19)$$

$$w' = U_* \left(A_{wy} e^{-B_{wy} Y} \right)^{\frac{Z}{Y+Z}} \left(A_{wz} e^{-B_{wz} Z} \right)^{\frac{Y}{Y+Z}} \quad (20)$$

$$f_v(Y) = \begin{cases} 1, & \text{if } Y \leq 0.6 \\ 1 - a(Y - 0.6)^2, & \text{else} \end{cases} \quad (21)$$

where $Y=(h-y)/h$, $Z=z/h$ and other variables are empirical constants equal as follows: $A_{vy}=0.9$, $B_{vy}=0.7$, $A_{vz}=1.3$, $B_{vz}=0.9$, $A_{wy}=1.4$, $B_{wy}=0.9$, $A_{wz}=1.0$ and $B_{wz}=0.7$. If the width of edge zone is different from the depth, formulae (19) – (21) are stretched to fit the chosen edge zone width by using relation $Z=z/\gamma L$ instead of that specified above.

Table 1. Experimental conditions in rectangular channel

Case	Dis-charge Q [l/s]	Depth h [m]	Width B [m]	Maximal velocity [m/s]	Energy gradient
S1	7.95	0.05	0.4	0.463	0.000937
S2	7.58	0.102	0.4	0.235	0.000138

It is assumed that Eqs.(19-21) are valid in the edge zones (in particular at vertical $z=\gamma L$) and Eqs.18 in the centerline of the chan-

nel (at vertical $z=B/2$). The turbulent stresses between these verticals are calculated from the following interpolating formulae:

$$v' = v' \Big|_{\gamma L} e^{-\alpha \frac{z-\gamma L}{B/2-\gamma L}} + v'_{2D} \left(1 - e^{-\alpha \frac{z-\gamma L}{B/2-\gamma L}} \right) \quad (22)$$

$$w' = w' \Big|_{\gamma L} e^{-\alpha \frac{z-\gamma L}{B/2-\gamma L}} + w'_{2D} \left(1 - e^{-\alpha \frac{z-\gamma L}{B/2-\gamma L}} \right) \quad (23)$$

Exponential interpolation between these verticals was adopted because possible changes in turbulent intensities occur closer to a side wall rather than to the channel centerline. The best result is achieved for $\alpha=8$. The calibrations were carried out for square edge zones.

Hydrodynamic model

The considered open channel is tilted in longitudinal direction, the bed slope is θ and all walls are rough. The flow is supposed to be steady with average velocity components (U , V , W) in the x , y and z directions, respectively. It is assumed that the turbulent transport of momentum in the x -direction is negligible. Therefore, the terms involving second derivatives with respect to x are negligible. This kind of flow is usually called parabolic in longitudinal direction. The basic equations describing the 3D velocity field in open channel flows are the continuity and momentum equations. Shear and normal turbulent stresses are defined separately. The shear stresses are expressed by Eq.11 and Eq.12 and the components of MLT by Eqs.(15-17). The components of the normal stresses are given by equations 18. All these equations form the hydrodynamic model of the three-dimensional turbulent flow in open channels.

$$\frac{\partial U^2}{\partial x} + \frac{\partial V U}{\partial y} + \frac{\partial W U}{\partial z} + \frac{1}{\rho} \frac{\partial P}{\partial x} = g \sin \theta + \frac{\partial}{\partial y} \left(\left[\frac{1}{2} S (l_x^2 + l_y^2) \right] \frac{\partial U}{\partial y} \right) + \frac{\partial}{\partial z} \left(\left[\frac{1}{2} S (l_x^2 + l_z^2) \right] \frac{\partial U}{\partial z} \right) \quad (24)$$

$$\frac{\partial V U}{\partial x} + \frac{\partial V^2}{\partial y} + \frac{\partial W V}{\partial z} + \frac{1}{\rho} \frac{\partial P}{\partial y} = g \cos \theta + \frac{\partial(-\overline{v^2})}{\partial y} + \frac{\partial}{\partial z} \left(\left[\frac{1}{2} S (l_y^2 + l_z^2) \right] \left[\frac{\partial V}{\partial z} + \frac{\partial W}{\partial y} \right] \right) \quad (25)$$

$$\frac{\partial W U}{\partial x} + \frac{\partial W V}{\partial y} + \frac{\partial W^2}{\partial z} + \frac{1}{\rho} \frac{\partial P}{\partial z} = \frac{\partial(-\overline{w^2})}{\partial z} + \frac{\partial}{\partial y} \left(\left[\frac{1}{2} S (l_y^2 + l_z^2) \right] \left[\frac{\partial V}{\partial z} + \frac{\partial W}{\partial y} \right] \right) \quad (26)$$

where P is the total pressure, i.e., the sum of the pressure resulting from the normal components of the molecular forces and the pressure arising from nonisotropic turbulence[2].

To solve the above set of equations, the numerical parabolic procedure known as Patankar-Spalding algorithm is used. It solves the set of the above equations for three components of velocity U , V , W and pressure P , at each forward step in longitudinal direction. The continuity equation (Eq.1) is solved for the pressure using the well known Patankar-Spalding algorithm. Boundary conditions for streamwise velocity were specified by wall-function approach [6]. At a free surface, the normal gradient of U is assumed to be zero. However, this condition may be rectified near side walls by taking into account experimental data. Measurements in both cases, S1 and S2, (table 1) show explicitly non-zero values for normal gradient of streamwise velocity at the water surface up to twice depth distance from a side wall. Experimental distribution of $\partial U/\partial y$ at free surface in each case can be approximated fairly well by the following equation

$$\frac{\partial u}{\partial y}(\zeta) = \begin{cases} u_{\max} = 0.4(2-\zeta)\zeta, & \text{if } \zeta < 2 \\ 0 & \text{else} \end{cases} \quad (27)$$

where $\zeta=d/h$, and d is a distance from a surface point to the nearest side wall. Slip conditions were set for secondary velocities. The cross section was covered with a 24x50 grid. All computations were run till obtaining a fully developed flow. It typically needed about 1200 forward steps and 15 min CPU time on PC Pentium-133.

Numerical model and simulations

The numerical procedure described above was applied to simulate 3D velocity field in an open channel flow for some experimental data published by Tominaga et al. [14]. These data concern the primary velocity distributions, the secondary current patterns and the intensities of turbulence in the cross section of the channel. The latter were used to define the turbulent normal stresses in an open channel.

The main objective of the numerical simulations is to show how the model describes the 3D velocity field in open channel flows for different structures of turbulence. The structure is defined by the following factors:

- The main components of the mixing length tensor given at each point of the channel cross-section.
- The size (width) of the edge zone which depends on the bed friction-effect [15].
- The distribution of turbulence intensities in the cross-section of the channel.

The structure is defined also by the sizes of turbulent eddies because of the relation between the mixing lengths and the sizes of the largest turbulent eddies. The model enables calculation of streamwise velocity distributions as well as secondary currents in open channel flows. Presumably distributions of streamwise velocity in a cross-section mainly depend on the first two factors, i.e., the mixing lengths and the width of the edge zone. The pattern of secondary currents in the channel cross-section depends mainly on the distribution of turbulence intensities in the edge

zones. In the case of isotropic distribution of turbulence intensities, the transversal components of mean velocity are zeros. Numerical simulations have confirmed these suppositions.

All numerical simulations were carried out for the distribution of intensities of turbulence defined by Eqs 18 through 23 with all coefficients being constant. These coefficients were verified in many numerical calculations and they are treated as universal constants. Preliminary results of numerical simulations show that the width of the edge zone should not much differ from the depth of water flow for considered open channel flows. Thus, all the numerical simulations discussed below were performed for the square edge zone only.

Figures 2 and 3 show streamwise velocity contour and secondary currents for the square edge zone in which the mixing length ellipsoid (MLE) is stretched in the longitudinal direction in the same way, i.e., $l_x/l_y=2$. The only difference is in the aspect ratio for mixing length ellipsoid, namely $l_z/l_y=1.42$ (wide ellipsoid, Fig.2) and $l_z/l_y=0.5$ (narrow ellipsoid, Fig.3). It is easy to notice that the narrow MLE produces much stronger vortex (the maximum speed $U_{s,m} \approx 0.43\text{cm/s}$) than the wider MLE ($U_{s,m} \approx 0.27\text{cm/s}$) does. A comparison of the streamwise velocity distributions for these two MLE patterns shows that isovels indicate enlarging of a zone with little gradients at some distance from the side wall for smaller l_z . If l_z comes to zero, effective viscosities in motion equations for V and W velocity components become smaller, so that both secondary velocity components grow up, producing more intensive secondary current. This current, in turn, influences

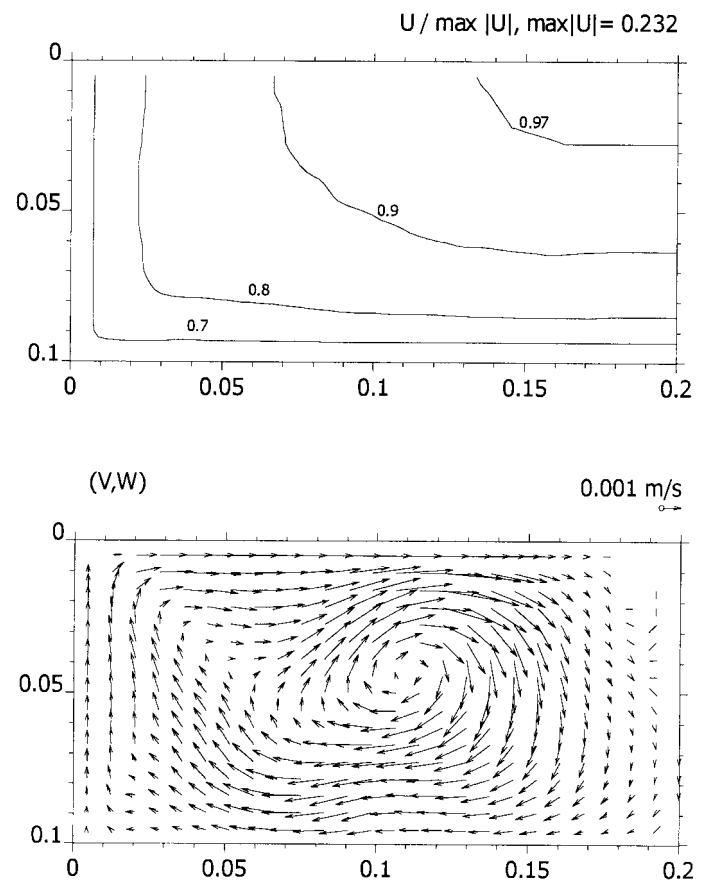


Fig. 2. Streamwise velocity contour lines and secondary currents for $l_x : l_y : l_z = 2 : 1 : 1.42$.

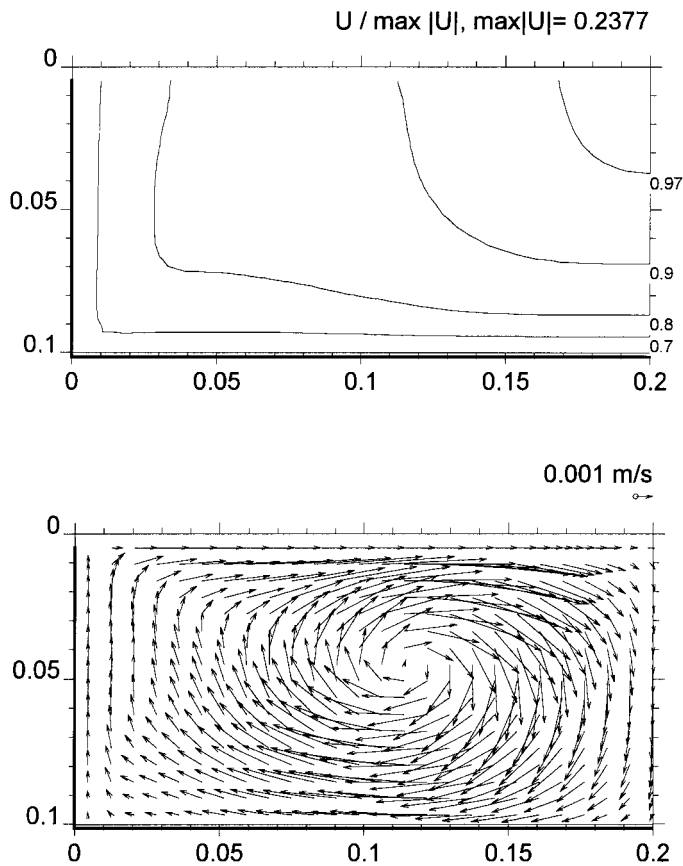


Fig. 3. Streamwise velocity contour lines and secondary currents for $l_x : l_y : l_z = 2 : 1 : 0.5$.

streamwise velocity distribution driving the low momentum fluid in the subsurface layer from the side wall to the center of the channel. The reference experimental data support the square edge zone with the mixing length ellipsoid $l_x : l_y : l_z = 2 : 1 : 1.42$. Figures 3, 4 and 5 display isovels of streamwise velocity and secondary currents vectors for square edge zone with different mixing length ellipsoids. The ratios of main axes of ellipsoids are 2:1:0.5, 4.5:1:0.5 and 7:1:0.5, respectively. The last case represents a very stretched MLE in the longitudinal direction. It is interesting that the largest turbulent eddies related to this case have main sizes equal to 1.4h in the longitudinal direction, 0.2h in the vertical direction and 0.1h in the lateral direction. The secondary current patterns as well as the distributions of streamwise velocity are almost the same in last two cases. This is understandable because the mixing length, l_x prevails in these cases and contributions of l_y and l_z into effective viscosities are insignificant. The secondary current vortex is a little stronger for more stretched ellipsoid, and it is a little shifted towards the channel centerline. One can notice that growth of ratio $l_x : l_y$ actually means a decrease of l_y . When $l_x : l_y$ goes from 2 to 7, the absolute value of l_x rises only about 11% up whereas l_y becomes approximately 3 times less. Little changes in eddy viscosity coefficients actually allow isovels picture to hold similar. The smaller l_y and l_z result in the smaller eddy viscosity in equations for V and W (Eqs. 25-26), and this in turn produces the greater values of V and W. Near the corners of the channel, where l_y and l_z are very small, additional tiny weak whirls appear.

Summary and conclusions

The presented model takes into account some subtle effects appearing in the open channel turbulent flows which can be modeled by differences between various components of turbulent stress tensor. Contrary to the very general models incorporating differential or algebraic equations for individual Reynolds stresses, it is relatively simple. It comprises only a few parameters to assign. The most important is the intensity of turbulence and the mixing lengths. The first one is easy to measure today, while the second one is well known by engineers. The model is easy to calibrate by choosing the mixing length sizes. It allows to produce a relatively simple secondary flow structure (one vortex) as well as more complicated ones (a main vortex and bottom vortex, see Fig.4 and Fig.5). In addition, it permits to produce in a sub-surface layer the so called velocity deep phenomenon by choosing a suitable boundary condition at free-surface (equation 27).

It can be difficult to define the mixing length ellipsoid (MLE) in the cross-section of open channels, especially in the channel corner. The presented formulae for generic mixing length and main components of MLE can only be adopted for channels which are similar to the channel discussed above. Other channels need some calibration procedure to find out all parameters of the presented model. The results of the performed numerical simulations reveal some important features of MLE in producing the streamwise velocity distribution as well as the secondary flow. The most important of these are listed below:

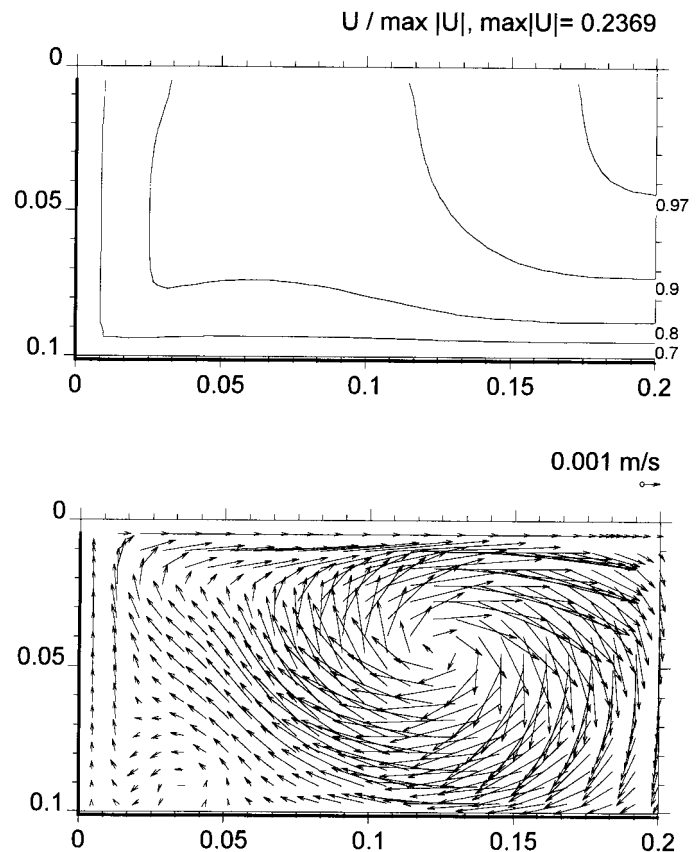


Fig. 4. Streamwise velocity contour lines and secondary currents for $l_x : l_y : l_z = 4.5 : 1 : 0.5$.

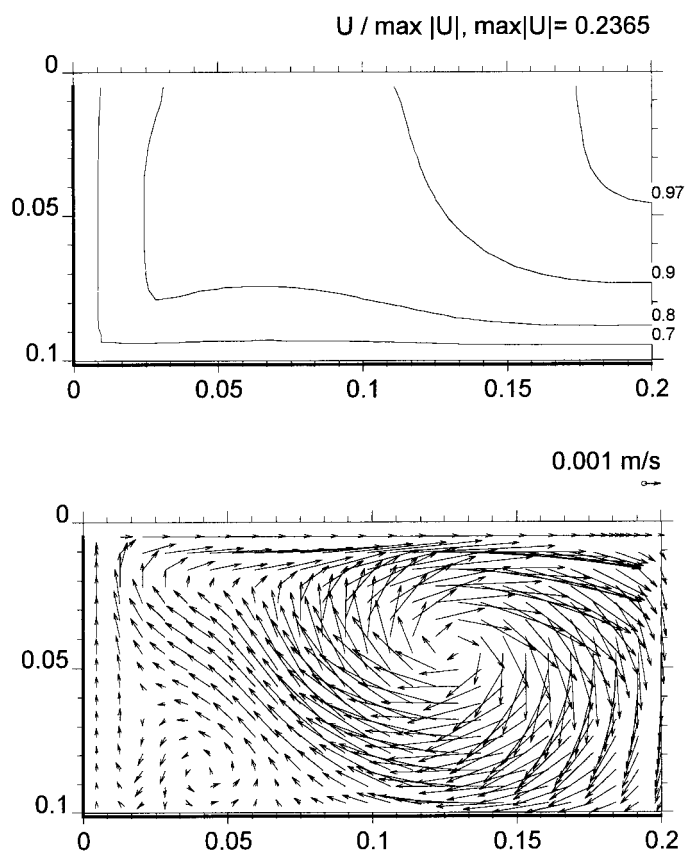


Fig. 5. Streamwise velocity contour and secondary currents for $l_x : l_y : l_z = 7 : 1 : 0.5$.

- The width of the edge zone should not much differ from the depth of water flow, then there is one strong vortex in the half of the channel. The choice of wider edge zones causes the decrease of influence of the side walls on velocity distributions in the cross-section of the channel. Choosing the narrow edge zone causes the opposite, the role of a side wall is overestimated.
- The narrow MLE and wide MLE for square edge zone produce very similar secondary current patterns with one vortex but with different strengths. The narrow MLE produces much stronger vortex than the wider MLE.
- Stretching MLE in longitudinal direction in the range $l_x/l_y=4.5-7$, does not cause any big changes in streamwise velocity distributions as well as in secondary current patterns. The vortex becomes weaker for small stretching MLE ($l_x/l_y=2$) and more shifted towards the channel side wall. For stretching the longitudinal axis of ellipsoid in excess of 4.5, an additional bottom vortex appears near the channel corner.

References

1. BRADSHAW, P. (1987). 'Turbulent secondary flows.' *Advances in Hydro-Science and-Engineering*, 19(3), 53-74.
2. CZERNUSZENKO, W. and RYLOV, A. A. (2000). 'A generalisation of Prandtl's model for 3D open channel flows.' *Journal of Hydraulic Research*, 38(2), 133-139.
3. GERARD, R. (1978). 'Secondary flow in noncircular conducts.' *Journal of the Hydraulics Division*, 104 (HY5), 755-773.

4. GESSNER, F. B. (1972). 'The origin of secondary flow in turbulent flow along a corner.' *Journal Fluid Mechanics*, 58(1), 1-25.
5. GESSNER, F. B. and JONES, J. B. (1965). 'On some aspects of fully-developed turbulent flow in rectangular channels.' *Journal of Fluid Mechanics*, 23(Part 4), 689-713.
6. LAUNDER, B.E. and SPALDING, D. B. (1974). 'The numerical computation of turbulent flows.' *Computer Methods in Applied Mechanics and Engineering*, 3, 269-
7. MONIN, A. S. and YAGLOM, A. M. (1971). *Statistical Fluid Mechanics-Mechanics of Turbulence*. MIT Press, Cambridge, Massachusetts.
8. NEZU, I. and NAKAGAWA, H. (1993). *Turbulence in Open-Channel Flows*. A.A.Balkema, Rotterdam.
9. NEZU, I. and RODI, W. (1986). 'Open-channel flow measurements with a laser doppler anemometer.' *Journal of Hydraulic Engineering*, 112(5), 335-355.
10. PERKINS, H. J. (1970). 'The formation of streamwise vorticity in turbulent flow.' *Journal of Fluid Mechanics*, 44(Part 4), 721-740.
11. POLLARD, A. (1989). 'Comparative Study of Turbulence Models in Predicting Turbulent Pipe Flow; Part 2: Reynolds Stress and k-e Models.' *AIAA Journal*, 27(12), 1714-1721.
12. RODI, W. (1980). *Turbulence models and their application in hydraulics*. University of Karlsruhe, Karlsruhe.
13. Schlichting, H. (1968). *Boundary-layer theory*. Pergamon Press, London.
14. TOMINAGA, A., Nezu, I., Ezaki, K, and Nakagawa, H. (1989). 'Three-dimensional turbulent structures in straight open channel flows.' *Journal of Hydraulic Research*, 27(1), 149-173.
15. YALIN, M. S. (1992). *River Mechanics*. Pergamon Press, Oxford.

Notation

$A(d)$	= greatest size of turbulent eddies at the given vertical in 2D approach;
$A_{vy}, A_{vz}, A_{wy}, A_{wz}$	= empirical constants;
$B_{vy}, B_{vz}, B_{wy}, B_{wz}$	= empirical constants;
$C_k, D_i (i=1,2,3)$	= empirical constants;
d	= z-distance from the side wall as shown in Fig.1;
D_{ij}	= deformation rate tensor;
l	= Prandtl's mixing length;
l_{ij}	= mixing length tensor;
l_x, l_y, l_z	= main components of the mixing length tensor;
L	= greatest size of turbulent eddies in 2D approach;
L_x, L_y, L_z	= lengths of the principal axes of the largest turbulent eddies;
p, q_y, q_z	= empirical coefficients.
U_i	= i-th component of the mean velocity (also U, V, W are used)
u_i	= i-th component of the turbulent velocity (also notation u, v, w are used)

u',v',w'	= intensities of turbulence in longitudinal, vertical and lateral direction respectively.	ζ	= non-dimensional lateral distance from the side wall
x,y,z	= coordinate system (x- longitudinal, y- vertical, z- lateral direction)	Θ	= bed slope
y	= distance from the water surface	μ	= coefficient of viscosity
Y	= $(h-y)/h$;	ν	= kinematic coefficient of viscosity
Z	= z/h	ν_t	= turbulent viscosity
γ	= parameter which defines the width of the edge zone;	ν_{ij}	= tensor of turbulent viscosity
		ξ	= $(h-y)/h$
		$\Omega_x, \Omega_y, \Omega_z$	= components of mean vorticity vector